Biophys Rep 2020, 6(4):137–145
https://doi.org/10.1007/s41048-020-00110-1

Biophysics Reports

METHOD

Measurement of viscoelastic properties of injured mouse brain after controlled cortical impact

Yu Chen[1], Suhao Qiu[1], Cheng Wang[2], Xiaowei Li[3], Yaohui Tang[2], Yuan Feng[1]✉

[1] Institute for Medical Imaging Technology, School of Biomedical Engineering, Shanghai Jiao Tong University, Shanghai 200030, China
[2] School of Biomedical Engineering and Med-X Research Institute, Shanghai Jiao Tong University, Shanghai 200030, China
[3] Bio-ID Center, School of Biomedical Engineering, Shanghai Jiao Tong University, Shanghai 200240, China

Received: 1 April 2020 / Accepted: 24 June 2020 / Published online: 1 August 2020

Abstract Mechanical properties of brain tissue can provide vital information for understanding the mechanism of traumatic brain injury (TBI). As mouse models were commonly adopted for TBI studies, a method to produce injury to the brain and characterize the injured tissue is desired. In this paper, a complete workflow of TBI induction, sample preparation, and biomechanical characterization is presented for measurement of the injured brain tissue. A controlled cortical impact device was used to induce injury to the brain. By setting the angle, speed, and position of the impact, the level of brain injuries could be controlled. Viscoelastic properties of both injured and non-injured brain tissues were measured using a ramp-hold indentation test. Regions of interests (ROIs) were tested and compared to contralateral corresponding counterparts. Methods introduced in this paper could be easily extended to produce and test a variety of other injured soft biological tissues.

Keywords Controlled cortical impact, Traumatic brain injury, Viscoelastic properties, Mouse model

INTRODUCTION

Traumatic brain injury (TBI) is one of the major causes of morbidity and mortality worldwide, with more than 50 million patients each year and causing 400 billion dollars of global economy loss annually (Maas *et al*. 2017). TBI is induced by a mechanical process. Many studies have shown that mechanical properties of the brain are closely related to its development and diseases (Goriely *et al*. 2015). Biomechanical testing of the brain tissue could provide key physical parameters for the modeling and prediction of TBI (Ganpule *et al*. 2017; Lu *et al*. 2019; Madhukar and Ostoja-Starzewski 2019; Zhao *et al*. 2017; Zhou *et al*. 2019). Comparisons of mechanical properties between the healthy and injured brain tissues can provide important clues to understand the mechanism of TBI (Feng *et al*. 2017a; Qiu *et al*. 2020). Therefore, understanding the biomechanical properties of the brain tissue is important to decipher the myths of TBI.

Animal models are indispensable for TBI research since injury-level experiments are impractical for human subjects. Despite the fact that the animal models cannot completely represent human brain injury, animal models of TBI still offer the best alternative to examine the biomechanical, cellular, and molecular mechanism of TBI-associated neuropathological progression (Ma *et al*. 2019). Animal models such as pig (Pasquesi and Margulies 2018), mouse (Chen *et al*. 2014), and monkey (King *et al*. 2010) have been used for TBI studies. Among them, mouse model is relatively easy to implement and provides various genetic manipulation options for translational studies. To induce brain injury, typical techniques include blast wave, weight-drop,

✉ Correspondence: fengyuan@sjtu.edu.cn (Y. Feng)

lateral fluid percussion, and control cortical impact (CCI). The blast wave technique is usually carried out in closed skull, inducing severe brain injuries. It is relatively difficult to carry out and hard to quantify. The other three methods are generally carried out under the condition of open skull and the injury is relatively easy to quantify. The weight-drop method is straightforward to conduct, but can only mimic a vertical impact on brain. The lateral fluid percussion method is usually used to induce diffuse axonal injury (DAI), but the speed of water is hard to control. The CCI method uses electric or pneumatic devices to induce injuries via a striking tip. It provides the best control of impact velocity, depth, and direction and thus the best control of injury levels. However, CCI is only suitable for small animals. Therefore, we adopted an *in vivo* mouse model to investigate the injured brain tissue using CCI.

To acquire the biomechanical properties of the brain tissue, many different methods have been adopted to characterize the brain tissue (Goriely *et al*. 2015). Tension tests (Rashid *et al*. 2012), shear tests (Destrade *et al*. 2015; Rashid *et al*. 2013), and indentation tests (Budday *et al*. 2015; Feng *et al*. 2017b; van Dommelen *et al*. 2010; MacManus *et al*. 2017a) were the mostly used. Tension tests such as uniaxial or biaxial tests could provide uniform deformation, facilitating measurements backed by analytical models. Shear tests can also provide uniform shear deformation and a direct measurement of the shear modulus. However, both tension and shear tests require the sample to be properly fixed at the boundaries. This poses a great challenge for brain tissue. In addition, it is especially challenging to conduct tension or shear tests on a specific region of brain. Indentation does not need special fixations for samples. Therefore, it provides a great convenience for testing brain tissue. In addition, indentation tests have also shown to be effective in testing specific regions in various scales (Hu *et al*. 2020; Qiu *et al*. 2020).

In this method study, viscoelastic properties of the brain tissue after CCI were measured using indentation. Both the CCI and indentation devices were custom-built. As a demonstration of method, we induced mild injuries to the mouse brain. Two regions of interests (ROIs), the cortex and hippocampus, were tested in both the ipsilateral and contralateral hemisphere. The proposed method of viscoelastic characterization was not limited to measure brain tissue, but could also be used to measure any soft biological tissues.

EXPERIMENTAL SECTION

CCI device

A custom-built CCI device was built for inducing injury to the mouse brain. It has a cylindrical tip to produce impact on the mouse brain (Fig. 1). The impact motion was generated using a voice coil (SMAC Corporation, Carlsbad, California, USA). The impact speed and acceleration were controlled using an industrial workstation (LCC-10 controller). The workstation was connected to the voice coil as a control console. The impact angle was adjusted with an angle dial gauge. To fix the mouse head firmly, a stereotaxic head frame was placed under the voice coil, with its center aligned along the impact tip. A custom-written program (based on SMAC LAC-X Editor V1.0) was used to control the impact speed.

Indentation device

A custom-built indentation device was used to characterize the viscoelastic properties of the brain tissue. The indentation motion was produced with an electric motor (SMAC Corporation, Carlsbad, California, USA). A cylindrical indenter with a flat tip and a diameter of 2 mm was rigidly connected to the motor for indentation (Fig. 2). A laser reflection plate was used for displacement measurement. The motion of the indenter was recorded with a laser sensor (Model HG-C1050 30 mm, Panasonic, Japan). A load cell (GSO-10, Transducer Technique, USA) connected to the indenter tip was used to measure the reaction force during the indentation. Signals from the sensors were collected with a data acquisition board (PCI-1706U, Advantech Co., Ltd., China) at a sampling rate of 1 kHz. A graphical user interface (GUI) based on LABVIEW (National Instruments, TX, USA) was designed for data acquisition and indentation control (Fig. 2).

Measurement protocol

Female mice (balb/c, 20 g, SPF grade, certificate No. SCXK 2018-0006) were used for demonstrating the protocol. For the open-skull impact, each mouse was anesthetized with chloride hydrate (10% concentration). After shaving hairs on the top of mouse head, a 5-mm-diameter trephine (Roboz Surgical Instrument Co., Gaithersburg, MD, USA) was used for craniotomy. Taking the left hemisphere as an example, the ROIs were chosen at the left rear of the anterior fontanel, about 3 mm to the left of the midline of skull. A circular shaped bone flap with a diameter of 3 mm was removed

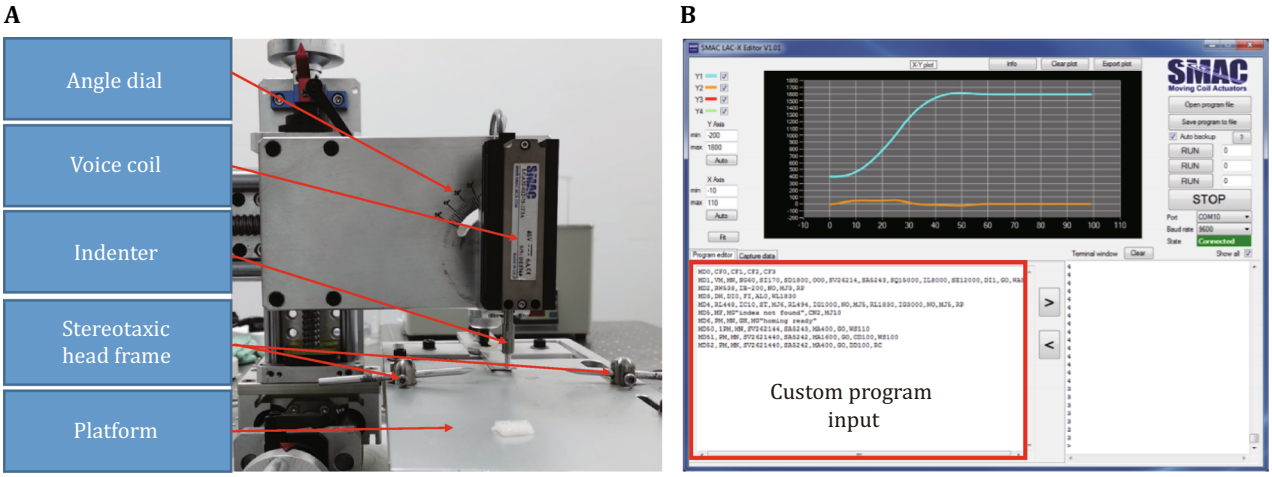

Fig. 1 **A** The custom-built CCI device to introduce injury to mouse brains. The impact angle is adjusted by an angle dial. The mouse head is fixed using a stereotactic frame. **B** The user interface of the software used to control the CCI device. The impact acceleration, velocity, and displacement can be controlled using custom-written programs

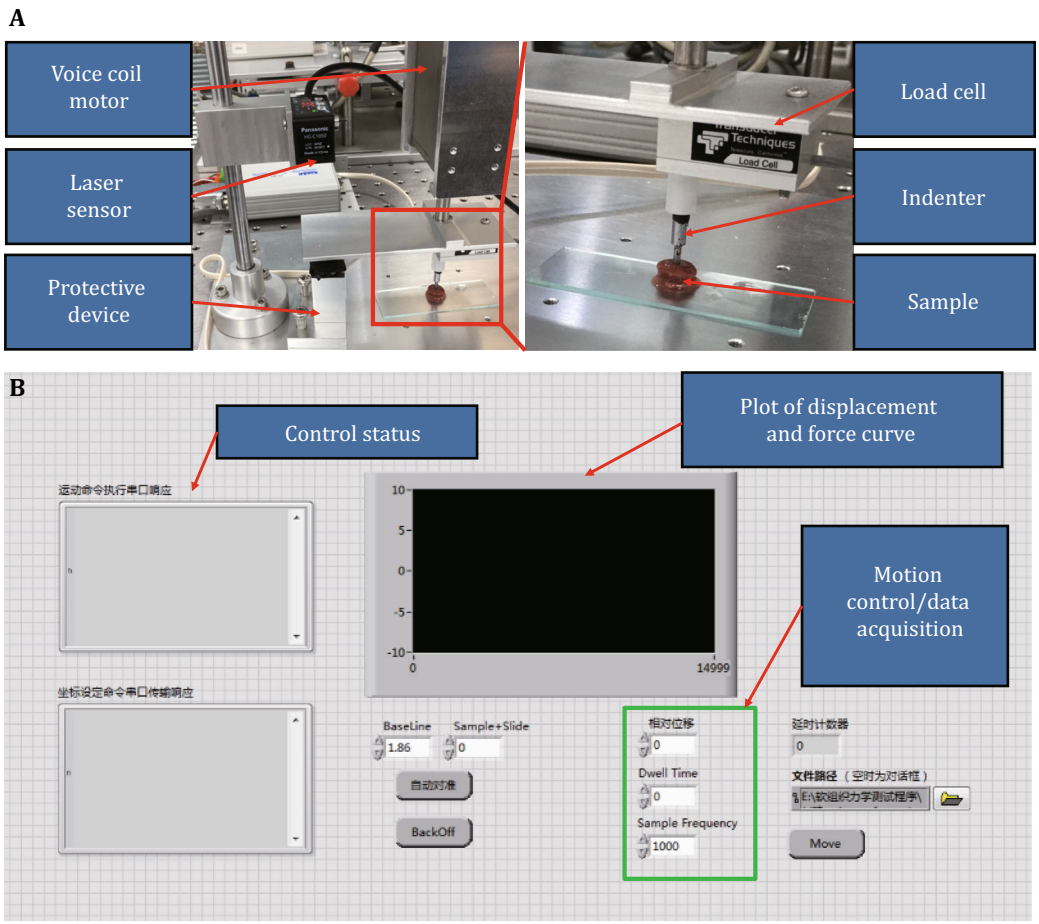

Fig. 2 **A** The custom-built indentation device. The motion of the indenter is recorded with the laser sensor. The reaction force is measured by the load cell connected to the indenter tip. **B** The custom-written graphic user interface (GUI) for device control. Indentation parameters such as depth, dwell time, and sample frequency can be input interactively. The displacement and force curves are updated in real time on the graph window during the test

to expose the ROIs after the craniotomy (Fig. 3). The skin wrapping the skull was peeled off after the mouse was anesthetized (Fig. 3). The impact position was taken at the middle of bregma and lambda with a 1.5 mm lateral distance on the left hemisphere. The ROIs were delineated on the skull before impact.

A cylindrical impact head with a diameter of 4 mm was fixed to the voice coil motor to produce the controlled impact. To avoid severe brain injury and skull rupture, the impact velocity was set to be less than 2 m/s and the controlled depth of the impact was about 1 mm for close-skull CCI. After CCI, the skin incision was sutured with a curved needle and the animals were housed in warm and clean environment supplied with food and water to reduce infection and mortality.

The brain was removed from skull before indentation test. Along the midline of skull, the skin wrapping the skull was cut to expose the skull. A small scissor was used to cut the soft tissue along the medullary foramen until it touched the skull. Then small slit was cut at the end of midline of the skull and the skull was peeled off carefully with forceps to expose the mouse's brain. Once the dissection was done, the whole brain could be removed from the skull.

Coronal slices of the brain were sectioned with a coronal slicing matrix (RWD Life Science, Shenzhen, China). Each slice was about 3 mm thick. The slice was stored in phosphorous-buffered saline (PBS) shortly before the indentation test. The pH value of the PBS solution (MA0015, Meilun Biotechnology, Dalian, China) was between 7.2 and 7.4. In this method study, four ROIs were chosen for comparative analysis as a demonstration: left cortex (LC), left hippo (LH), right cortex (RC), and right hippo (RH) (Fig. 3).

The indentation test includes five steps: (1) Measurement of the slice thickness. The distances with and without the sample were recorded by the laser sensor. The difference of the two measurements was taken as the thickness of the slice. (2) ROI selection. The selected ROI for measurement was placed directly below the indenter. (3) Contact. The indenter was lowered to be in contact with the sample surface. (4) Indentation. Each sample was indented within 8% of its sample thickness to minimize the boundary effect (Budday *et al*. 2015). Relaxation was followed for measurement of viscoelastic properties. The displacement and reactive force were recorded for 180 s since the start of the indentation. (5) All the recorded data were saved.

A flow chart of the protocol is summarized in Fig. 4. The CCI and indentation control, data acquisition, and result visualization were all carried out using a single PC (Fig. 5). A custom-written GUI was used to control all instrument, and the data communication was done via RS-232 ports.

Estimation of viscoelastic parameters

The displacement of indenter during ramp-hold test protocol is a piecewise function:

$$h(t) = \begin{cases} Vt & (0 \le t \le t_R) \\ Vt_R & (t_R \le t) \end{cases}, \quad (1)$$

where V is the indentation velocity and t_R is the indentation ramp time. Therefore, the corresponding reaction force based on 2-term Prony series is (Qiu *et al*. 2018) given as follows:

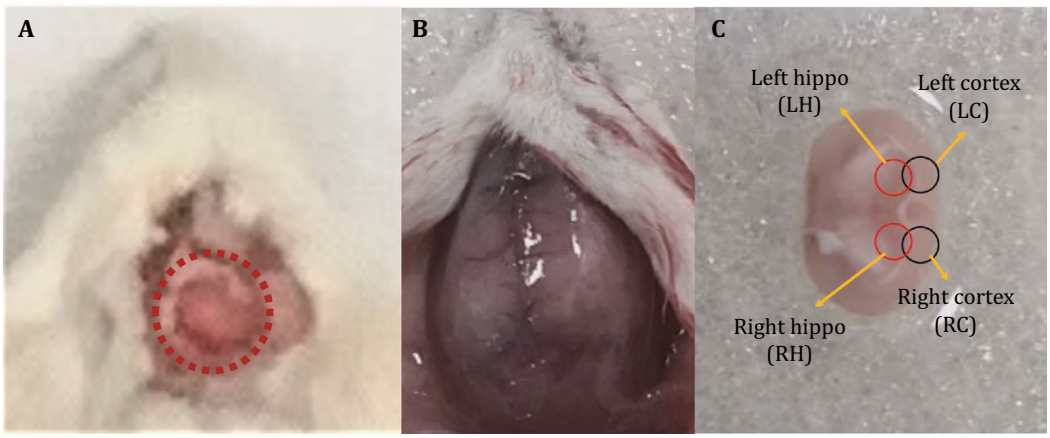

Fig. 3 **A** A mouse head prepared for an open-skull CCI. The red dotted circle indicates a piece of bone flap removed before impact. **B** A close-skull CCI setup. The skin was peeled before impact. **C** Typical ROIs selected for indentation tests on a slice of brain tissue

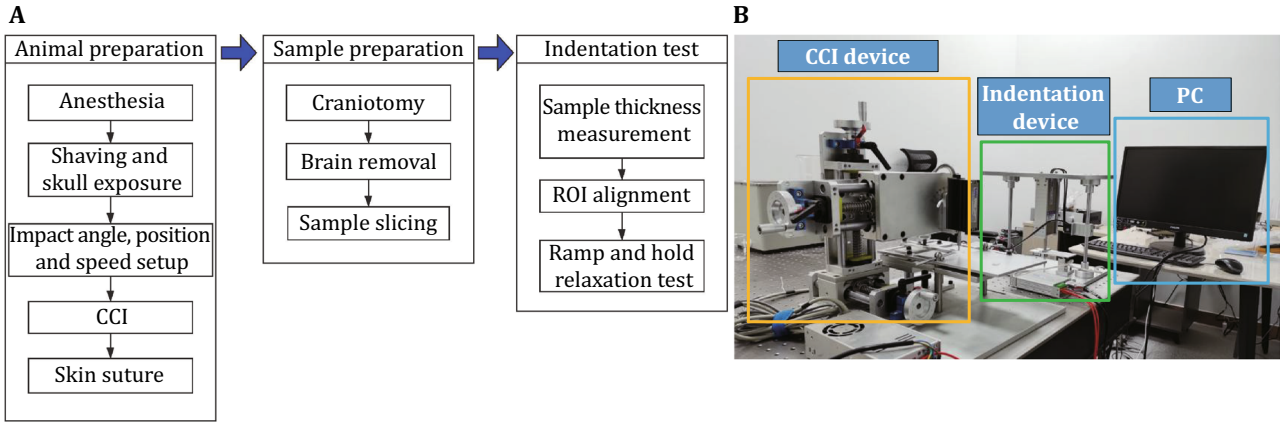

Fig. 4 **A** A flowchart showing detailed steps of this protocol. **B** An overview of the measurement devices for measuring viscoelastic properties of injured brain tissue. A personal computer (PC) was used for device control and data acquisition

$$F = \begin{cases} 8RXV\left(C_0 t - \sum_{i=1}^{2} \tau_i C_i \left(e^{-\frac{t}{\tau_i}} - 1\right)\right) & (0 \le t \le t_R) \\ 8RXV\left(C_0 t_R + \sum_{i=1}^{2} \tau_i C_i e^{-\frac{t}{\tau_i}} \left(e^{\frac{t_R}{\tau_i}} - 1\right)\right) & (t_R \le t) \end{cases}, \tag{2}$$

$$X = 1 + 1.133\left(\frac{\sqrt{Rh}}{H}\right) + 1.283\left(\frac{\sqrt{Rh}}{H}\right)^2 + 0.769\left(\frac{\sqrt{Rh}}{H}\right)^3 + 0.0975\left(\frac{\sqrt{Rh}}{H}\right)^4, \tag{3}$$

where R is the radius of the indenter, C_0, C_i and τ_i are components of Prony series, X represents the compensation factor (Dimitriadis *et al.* 2002), and h and H are the displacement of indenter and the thickness of the sample, respectively.

The viscoelastic parameters were estimated by a custom-written MATLAB (Mathworks, Natick, MA, USA) code with an objective function:

$$f_{\text{obj}}(C_0, C_i, \tau_i) = \left[w_1 \sqrt{\frac{1}{n}\sum_{j=1}^{n} \left(F^j - F^j_{\text{exp}}\right)^2} \right]_{0 \le t \le t_R} + \left[w_2 \sqrt{\frac{1}{m}\sum_{k=1}^{m} \left(F^k - F^k_{\text{exp}}\right)^2} \right]_{t_R \le t} (i = 1, 2), \tag{4}$$

where w_1 and w_2 were taken as 0.5. The n and m are the number of data points in each section. The corresponding instantaneous shear modulus G_0 and long-time shear modulus G_∞ are given as follows:

$$G_0 = G(0) = C_0 + \sum_{i=1}^{2} C_i, \tag{5}$$

$$G_\infty = G(\infty) = C_0. \tag{6}$$

RESULTS

Typical experimental and fitted force vs. time curves were shown in Fig. 5. As an illustration, the estimated viscoelastic model parameters for the four ROIs 1 h post injury are summarized (Table 1). A comparison of G_0 and G_∞ values is shown in Fig. 6. We observed higher mean G_0 values of LC and LH (1.31 kPa, 1.35 kPa), compared to that of RC and RH (1.02 kPa, 1.05 kPa). Student t-tests showed significant differences

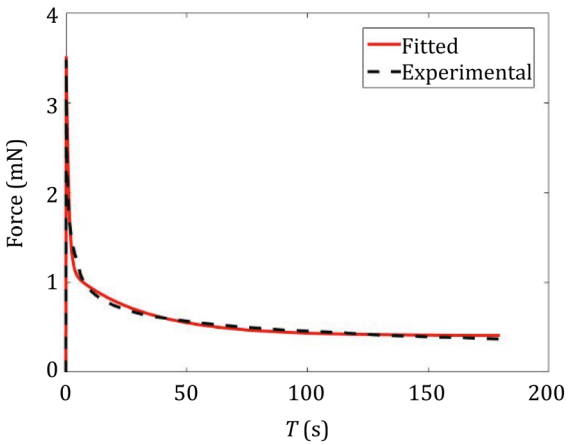

Fig. 5 Experimental and fitted force vs. time with 8% indentation strain. Brain samples were acquired from the injured cortex of the left hemisphere (LC) 1 h after close-skull CCI (impact velocity = 2 m/s, impact angle = 0°, R^2 = 0.96)

Table 1 Measured viscoelastic properties of the brain tissue 1 h post injury with 95% confidence intervals

	G_∞ (kPa)	C_1 (kPa)	C_2 (kPa)	τ_1 (s)	τ_2 (s)	G_0 (kPa)	R^2
Left cortex	0.12 ± 0.03	0.91 ± 0.31	0.28 ± 0.10	0.81 ± 0.15	27.87 ± 4.22	1.31 ± 0.42	0.96
Left hippo	0.16 ± 0.05	0.92 ± 0.49	0.26 ± 0.12	0.82 ± 0.16	26.64 ± 8.89	1.35 ± 0.65	0.96
Right cortex	0.11 ± 0.05	0.71 ± 0.33	0.20 ± 0.08	0.83 ± 0.14	26.20 ± 6.30	1.02 ± 0.46	0.96
Right hippo	0.13 ± 0.04	0.71 ± 0.40	0.21 ± 0.11	0.84 ± 0.14	22.75 ± 7.02	1.05 ± 0.54	0.97

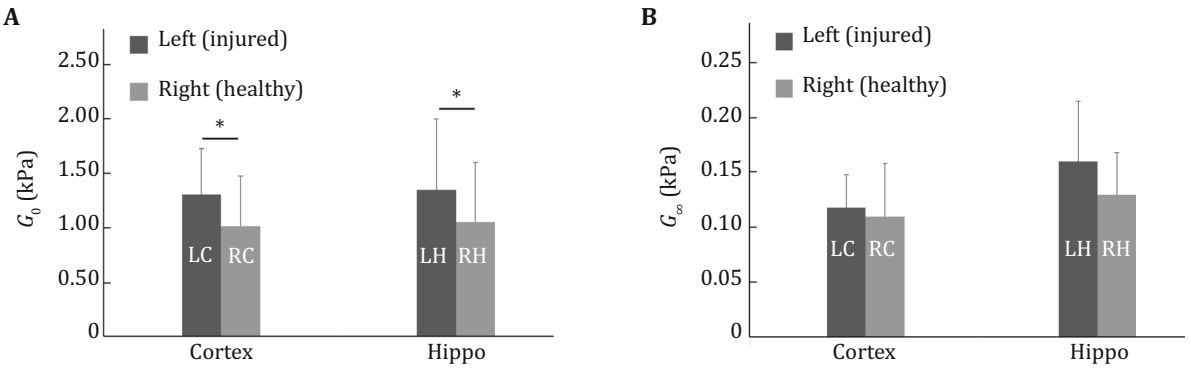

Fig. 6 Comparisons of G_0 (**A**) and G_∞ (**B**) values 1 h post injury. An asterisk indicates a significant difference between the healthy and injured pairs. "Left (injured)" indicates the left hemisphere that received impact. "Right (control)" indicates the right hemisphere without impact

($p < 0.05$) between LC/RC and LH/RH pairs in terms of G_0. However, the mean differences of the G_0 values between the two pairs were almost the same (0.29 kPa, 0.30 kPa). The G_∞ mean values of LC and LH (0.12 kPa, 0.16 kPa) were slightly higher than that of RC and RH (0.11 kPa, 0.13 kPa).

DISCUSSION

In this method, the CCI was introduced for producing injuries to the brain. The indentation test was used for measuring the viscoelastic properties of the brain tissue. By controlling the cortical impact magnitude and position, brain injuries with different levels and positions could be produced for a variety of TBI studies.

The impact depth and velocity are crucial parameters, although there is a wide range of impact velocities used in CCI studies, from 5–6 m/s (Lu and Mao 2019; Mao *et al*. 2013) to around 1 m/s. It is shown that for producing mild TBI in an open-skull condition, the impact depth and velocity should be less than 1 mm and 4 m/s, respectively (Ma *et al*. 2019). The impact velocities used here (1 mm depth and 2 m/s velocity) were similar to that of reported CCI studies using mouse model (Qiu *et al*. 2020; Toshkezi *et al*. 2018; Xu *et al*. 2019), producing mostly mild, no more than the moderate level of injury. Compared with the mice that did not receive CCI, the mice after CCI had a longer recovery time. In addition, the skull of the injured mice was intact and there was no obvious bleeding in the injured area. These experimental observations also confirmed the introduction of mild TBI.

With respect to the impact location, most animal studies focused on the area between lambda and bregma (Chen *et al*. 2014; Pleasant *et al*. 2011; Xu *et al*. 2014). This is because impacting this location could produce injury to hippocampus, cortex, and subcortical white matter simultaneously. The impact tip with a diameter of 4 mm was suitable for the brain of 8-week-old mouse. The 2-mm-diameter indenter tip could provide the best testing resolution for the small-sized mouse brain. In previous studies, we have also noticed that the impact angle significantly influenced instantaneous shear modulus after TBI (Qiu *et al*. 2020). Although most of the brain injury studies based on CCI adopted open-skull impact, 85%–89% of the TBI cases happened in closed skull (Myburgh *et al*. 2008). In this method study, we demonstrated the measurement protocol for inducing and measuring a mild injury. It should be noticed that the methods could be easily extended to testing brain tissues with different injury

levels with the corresponding impact velocity, depth, and angle.

Studies have shown that dynamic measurement could provide more information. However, dynamic testing poses additional challenges of measurements (MacManus *et al*. 2017a). Compared with the indirect measurement of slice thickness (Wang *et al*. 2020), a direct measurement using an independent laser sensor could be more accurate. However, one of the limitations is dehydration of the sample for viscoelastic measurement. For example, for a ramp-hold test, relaxation section could last as long as 3 min. A practical solution for preventing the dehydration is spraying PBS solution to the sample to keep it moisturized.

Among the many models proposed to characterize biomechanical properties of soft tissues (Holtzmann *et al*. 2016; Mijailovic *et al*. 2018; Sinkus *et al*. 2005), inverse method-based techniques could provide the best estimate (Feng *et al*. 2017b). However, computational cost of the inverse method was high. In addition, the inverse method could not provide instantaneous estimate. Models such as Quasi-linear neo-Hookean-based viscoelastic model offered better description in large deformations (Macmanus *et al*. 2017b), but could not be easily adopted for computation. The Prony series-based model adopted in this method was easy to implement and computationally efficient.

CONCLUSIONS

We introduced a method that could provide well-controlled velocity and angle for inducing impact injuries to specific brain regions using CCI. The indentation test procedure facilitated convenient sample preparation for brain tissue. By inducing a mild TBI to mouse brain, we demonstrated the method to measure the viscoelastic properties of both the injured and non-injured ROIs in the brain. Brain tissues with different injury levels could be produced by changing the impact speed and depth. In addition, it is easy to apply the indentation method to test other soft biological tissues such as liver, breast, and tumor.

Acknowledgment Funding support from National Natural Science Foundation of China (31870941) and Shanghai Science and Technology Committee (1944190700) are acknowledged. Technical assistance and helpful discussions from Jianhui Zhang and Dongjing Lu are acknowledged.

Compliance with Ethical Standards

Conflict of interest Yu Chen, Suhao Qiu, Chen Wang, Xiaowei Li, Yaohui Tang, and Yuan Feng declare that they have no conflict of interest.

Human and animal rights and informed consent All of the animal procedures and protocols were approved by the Institutional Animal Care and Use Committee of the Shanghai Jiao Tong University and all institutional and national guidelines for the care and use of laboratory animals were followed.

References

Budday S, Nay R, de Rooij R, Steinmann P, Wyrobek T, Ovaert TC, Kuhl E (2015) Mechanical properties of gray and white matter brain tissue by indentation. J Mech Behav Biomed Mater 46:318–330

Chen Y, Mao H, Yang KH, Abel T, Meaney DF (2014) A modified controlled cortical impact technique to model mild traumatic brain injury mechanics in mice. Front Neurol 5:100

Destrade M, Gilchrist MD, Murphy JG, Rashid B, Saccomandi G (2015) Extreme softness of brain matter in simple shear. Int J Non-Linear Mech 75:54–58

Dimitriadis EK, Horkay F, Maresca J, Kachar B, Chadwick RS (2002) Determination of elastic moduli of thin layers of soft material using the atomic force microscope. Biophys J 82(5):2798–2810

Feng Y, Gao Y, Wang T, Tao L, Qiu S, Zhao X (2017a) A longitudinal study of the mechanical properties of injured brain tissue in a mouse model. J Mech Behav Biomed Mater 71:407–415

Feng Y, Lee CH, Sun L, Ji S, Zhao X (2017b) Characterizing white matter tissue in large strain via asymmetric indentation and inverse finite element modeling. J Mech Behav Biomed Mater 65:490–501

Ganpule S, Daphalapurkar NP, Ramesh KT, Knutsen AK, Pham DL, Bayly PV, Prince JL (2017) A three-dimensional computational human head model that captures live human brain dynamics. J Neurotrauma 34(13):2154–2166

Goriely A, Geers MG, Holzapfel GA, Jayamohan J, Jerusalem A, Sivaloganathan S, Squier W, van Dommelen JA, Waters S, Kuhl E (2015) Mechanics of the brain: perspectives, challenges, and opportunities. Biomech Model Mechanobiol 14(5):931–965

Holtzmann K, Gautier HO, Christ AF, Guck J, Karadottir RT, Franze K (2016) Brain tissue stiffness is a sensitive marker for acidosis. J Neurosci Methods 271:50–54

Hu J, Chen S, Huang D, Zhang Y, Lü S, Long M (2020) Global mapping of live cell mechanical features using PeakForce QNM AFM. Biophysics Reports 6(1):9–18

J.A.W. van Dommelen, TPJ van der Sande, M. Hrapko, G.W.M. Peters (2010) Mechanical properties of brain tissue by indentation: Interregional variation. J Mech Behav Biomed Mater 3(2): 158–166

King C, Robinson T, Dixon CE, Rao GR, Larnard D, Nemoto CEM (2010) Brain temperature profiles during epidural cooling with the ChillerPad in a monkey model of traumatic brain injury. J Neurotrauma 27(10):1895–1903

Lu L, Mao H (2019) Quantifying the effect of repeated impacts and lateral tip movements on brain responses during controlled cortical impact. J Neurotrauma 36(11):1828–1835

Lu YC, Daphalapurkar NP, Knutsen AK, Glaister J, Pham DL, Butman JA, Prince JL, Bayly PV, Ramesh KT (2019) A 3D computational head model under dynamic head rotation and head extension validated using live human brain data, including the falx and the tentorium. Ann Biomed Eng 47(9):1923–1940

Ma X, Aravind A, Pfister BJ, Chandra N, Haorah J (2019) Animal models of traumatic brain injury and assessment of injury severity. Mol Neurobiol 56(8):5332–5345

Maas AIR, Menon DK, Adelson PD, Andelic N, Bell MJ, Belli A, Bragge P, Brazinova A, Büki A, Chesnut RM, Citerio G, Coburn M, Cooper DJ, Crowder AT, Czeiter E, Czosnyka M, Diaz-Arrastia R, Dreier JP, Duhaime A-C, Ercole A, van Essen TA, Feigin VL, Gao G, Giacino J, Gonzalez-Lara LE, Gruen RL, Gupta D, Hartings JA, Hill S, Jiang J-Y, Ketharanathan N, Kompanje EJO, Lanyon L, Laureys S, Lecky F, Levin H, Lingsma HF, Maegele M, Majdan M, Manley G, Marsteller J, Mascia L, McFadyen C, Mondello S, Newcombe V, Palotie A, Parizel PM, Peul W, Piercy J, Polinder S, Puybasset L, Rasmussen TE, Rossaint R, Smielewski P, Söderberg J, Stanworth SJ, Stein MB, von Steinbüchel N, Stewart W, Steyerberg EW, Stocchetti N, Synnot A, Te Ao B, Tenovuo O, Theadom A, Tibboel D, Videtta W, Wang KKW, Williams WH, Wilson L, Yaffe K, Adams H, Agnoletti V, Allanson J, Amrein K, Andaluz N, Anke A, Antoni A, van As AB, Audibert G, Azaševac A, Azouvi P, Azzolini ML, Baciu C, Badenes R, Barlow KM, Bartels R, Bauerfeind U, Beauchamp M, Beer D, Beer R, Belda FJ, Bellander B-M, Bellier R, Benali H, Benard T, Beqiri V, Beretta L, Bernard F, Bertolini G, Bilotta F, Blaabjerg M, den Boogert H, Boutis K, Bouzat P, Brooks B, Brorsson C, Bullinger M, Burns E, Calappi E, Cameron P, Carise E, Castaño-León AM, Causin F, Chevallard G, Chieregato A, Christie B, Cnossen M, Coles J, Collett J, Della Corte F, Craig W, Csato G, Csomos A, Curry N, Dahyot-Fizelier C, Dawes H, DeMatteo C, Depreitere B, Dewey D, van Dijck J, Đilvesi Đ, Dippel D, Dizdarevic K, Donoghue E, Duek O, Dulière G-L, Dzeko A, Eapen G, Emery CA, English S, Esser P, Ezer E, Fabricius M, Feng J, Fergusson D, Figaji A, Fleming J, Foks K, Francony G, Freedman S, Freo U, Frisvold SK, Gagnon I, Galanaud D, Gantner D, Giraud B, Glocker B, Golubovic J, Gómez López PA, Gordon WA, Gradisek P, Gravel J, Griesdale D, Grossi F, Haagsma JA, Håberg AK, Haitsma I, Van Hecke W, Helbok R, Helseth E, van Heugten C, Hoedemaekers C, Höfer S, Horton L, Hui J, Huijben JA, Hutchinson PJ, Jacobs B, van der Jagt M, Jankowski S, Janssens K, Jelaca B, Jones KM, Kamnitsas K, Kaps R, Karan M, Katila A, Kaukonen K-M, De Keyser V, Kivisaari R, Kolias AG, Kolumbán B, Kolundžija K, Kondziella D, Koskinen L-O, Kovács N, Kramer A, Kutsogiannis D, Kyprianou T, Lagares A, Lamontagne F, Latini R, Lauzier F, Lazar I, Ledig C, Lefering R, Legrand V, Levi L, Lightfoot R, Lozano A, MacDonald S, Major S, Manara A, Manhes P, Maréchal H, Martino C, Masala A, Masson S, Mattern J, McFadyen B, McMahon C, Meade M, Melegh B, Menovsky T, Moore L, Morgado Correia M, Morganti-Kossmann MC, Muehlan H, Mukherjee P, Murray L, van der Naalt J, Negru A, Nelson D, Nieboer D, Noirhomme Q, Nyirádi J, Oddo M, Okonkwo DO, Oldenbeuving AW, Ortolano F, Osmond M, Payen J-F, Perlbarg V, Persona P, Pichon N, Piippo-Karjalainen A, Pili-Floury S, Pirinen M, Ple H, Poca MA, Posti J, Van Praag D, Ptito A, Radoi A, Ragauskas A, Raj R, Real RGL, Reed N, Rhodes J, Robertson C, Rocka S, Røe C, Røise O, Roks G, Rosand J, Rosenfeld JV, Rosenlund C, Rosenthal G, Rossi S, Rueckert D, de Ruiter GCW, Sacchi M, Sahakian BJ, Sahuquillo J, Sakowitz O, Salvato G, Sánchez-Porras R, Sándor J, Sangha G, Schäfer N, Schmidt S, Schneider KJ, Schnyer D, Schöhl H, Schoonman GG, Schou RF, Sir Ö, Skandsen T, Smeets D, Sorinola A, Stamatakis E, Stevanovic A, Stevens RD, Sundström N, Taccone FS, Takala R, Tanskanen P, Taylor MS, Telgmann R, Temkin N, Teodorani G, Thomas M, Tolias CM, Trapani T, Turgeon A, Vajkoczy P, Valadka AB, Valeinis E, Vallance S, Vámos Z, Vargiolu A, Vega E, Verheyden J, Vik A, Vilcinis R, Vleggeert-Lankamp C, Vogt L, Volovici V, Voormolen DC, Vulekovic P, Vande Vyvere T, Van Waesberghe J, Wessels L, Wildschut E, Williams G, Winkler MKL, Wolf S, Wood G, Xirouchaki N, Younsi A, Zaaroor M, Zelinkova V, Zemek R, Zumbo F (2017) Traumatic brain injury: integrated approaches to improve prevention, clinical care, and research. Lancet Neurol 16(12):987–1048

MacManus DB, Pierrat B, Murphy JG, Gilchrist MD (2017a) Protection of cortex by overlying meninges tissue during dynamic indentation of the adolescent brain. Acta Biomater 57:384–394

MacManus DB, Pierrat B, Murphy JG, Gilchrist MD (2017b) A viscoelastic analysis of the P56 mouse brain under large-deformation dynamic indentation. Acta Biomater 48:309–318

Madhukar A, Ostoja-Starzewski M (2019) Finite element methods in human head impact simulations: a review. Ann Biomed Eng 47(9):1832–1854

Mao H, Elkin BS, Genthikatti VV, Morrison B 3rd, Yang KH (2013) Why is CA3 more vulnerable than CA1 in experimental models of controlled cortical impact-induced brain injury? J Neurotrauma 30(17):1521–1530

Mijailovic AS, Qing B, Fortunato D, van Vliet KJ (2018) Characterizing viscoelastic mechanical properties of highly compliant polymers and biological tissues using impact indentation. Acta Biomater 71:388–397

Myburgh JA, Cooper DJ, Finfer SR, Venkatesh B, Jones D, Higgins A, Bishop N, Higlett T (2008) Epidemiology and 12-month outcomes from traumatic brain injury in Australia and New Zealand. J Trauma Injury Infect Critical Care 64(4):854–862

Pasquesi SA, Margulies SS (2018) Measurement and finite element model validation of immature porcine brain-skull displacement during rapid sagittal head rotations. Frontiers Bioeng Biotechnol 6:16. https://doi.org/10.3389/fbioe.2018.00016

Pleasant JM, Carlson SW, Mao H, Scheff SW, Yang KH, Saatman KE (2011) Rate of neurodegeneration in the mouse controlled cortical impact model is influenced by impactor tip shape: implications for mechanistic and therapeutic studies. J Neurotrauma 28(11):2245–2262

Qiu S, Jiang W, Alam MS, Chen S, Lai C, Wang T, Li X, Liu J, Gao M, Tang Y, Li X, Zeng J, Feng Y (2020) Viscoelastic characterization of injured brain tissue after controlled cortical impact (CCI) using a mouse model. J Neurosci Methods 330:108463

Qiu S, Zhao X, Chen J, Zeng J, Chen S, Chen L, Meng Y, Liu B, Shan H, Gao M, Feng Y (2018) Characterizing viscoelastic properties of breast cancer tissue in a mouse model using indentation. J Biomech 69:81–89

Rashid B, Destrade M, Gilchrist MD (2012) Inhomogeneous deformation of brain tissue during tension tests. Comput Mater Sci 64:295–300

Rashid B, Destrade M, Gilchrist MD (2013) Mechanical characterization of brain tissue in simple shear at dynamic strain rates. J Mech Behav Biomed Mater 28:71–85

Sinkus R, Tanter M, Xydeas T, Catheline S, Bercoff J, Fink M (2005) Viscoelastic shear properties of in vivo breast lesions

measured by MR elastography. Magn Reson Imaging 23(2):159–165

Toshkezi G, Kyle M, Longo SL, Chin LS, Zhao L-R (2018) Brain repair by hematopoietic growth factors in the subacute phase of traumatic brain injury. J Neurosurg. https://doi.org/10.3171/2017.7.JNS17878:1-9

Wang M, Liu S, Xu Z, Qu K, Li M, Chen X, Xue Q, Genin GM, Lu TJ, Xu F (2020) Characterizing poroelasticity of biological tissues by spherical indentation: an improved theory for large relaxation. J Mech Phys Solids 138:103920. https://doi.org/10.1016/j.jmps.2020.103920

Xu SY, Liu M, Gao Y, Cao Y, Bao JG, Lin YY, Wang Y, Luo QZ, Jiang JY, Zhong CL (2019) Acute histopathological responses and long-term behavioral outcomes in mice with graded controlled cortical impact injury. Neural Regen Res 14(6):997–1003

Xu ZS, Yao A, Chu SS, Paun MK, McClintic AM, Murphy SP, Mourad PD (2014) Detection of mild traumatic brain injury in rodent models using shear wave elastography: preliminary studies. J Ultrasound Med 33(10):1763–1771

Zhao W, Cai Y, Li Z, Ji S (2017) Injury prediction and vulnerability assessment using strain and susceptibility measures of the deep white matter. Biomech Model Mechanobiol 16(5):1709–1727

Zhou Z, Li X, Kleiven S (2019) Fluid-structure interaction simulation of the brain-skull interface for acute subdural haematoma prediction. Biomech Model Mechanobiol 18(1):155–173